The local bearing capacity perpendicular to grain of structural timber elements

Construction and Building Materials 27 (2012) 54–59

Contents lists available at SciVerse ScienceDirect

Construction and Building Materials

journal homepage: www.elsevier.com/locate/conbuildmat

The local bearing capacity perpendicular to grain of structural timber elements

A.J.M. Leijten *, A.J.M. Jorissen, B.J.C. de Leijer [1]

University of Technology Eindhoven, Faculty of Architecture, Building and Planning, PO. Box 513, 5600 MB Eindhoven, The Netherlands

ARTICLE INFO

Article history:
Received 25 August 2010
Received in revised form 27 June 2011
Accepted 18 July 2011
Available online 28 September 2011

Keywords:
Timber
Engineering
Strength
Timber
Perpendicular to grain
Structural

ABSTRACT

The accuracy and reliability of empirical models for the local bearing capacity perpendicular to grain of timber beams is questionable as it is not based on any fundamental principal. This study shows that a physically based stress dispersion model can successfully be applied for a wide range of practical design situations. The credibility of this model is based on experiments, FEM and optical techniques used to assess and quantify the strength affecting parameters. This model is a potential candidate to be incorporated in future structural timber design standards.

1. Introduction

Many authors have reported compressive perpendicular to grain tests an issue as old as the structural problem of a simply supported beam. In the 19th century, with the introduction of the railway ties, many tests must have focused on the bearing resistance. In the early 20th century, engineered wood structures required knowledge of the bearing capacity caused by concentrated loads. An example can be found in timber light-frame construction where timber rails are supported and locally loaded by many transmitting studs as illustrated in Fig. 1. During those years, the permissible strength design method was based on the proportional strength limit, Kollmann/Côté [1]. An historic overview of some late 19th and early 20th century research efforts for the parameters that affect the bearing strength, are presented by Kühne [2]. Gehri [3], in his historic overview, focused on the relationship between compressive strength and timber density. Gehri argued that differences in the determination methods applied by the test standards around the globe, brought about leading to a confusing situation where test results become incompatible. On every continent, these incompatible test results are then used by empirical structural design models to determine the bearing capacity for a given structural detail. Regardless of which standards are used, the bearing capacity predicted should not differ too much, unless some models are more conservative than others. None of the empirical models consider the support condition of the beam subjected to concentrated loads. In fact, the complexity of the problem has forced many design codes' committees to accept an engineering approach.

Recently, a successful attempt was made to apply an elastic-fully plastic stress dispersion model to determine the bearing capacity, Van der Put [4]. Initially, the model explained the embedment capacity of dowel type fasteners in particle board. Later, it was applied to determine the bearing capacity of continuously supported timber beams, Fig. 2. The slope of the dispersing stresses depends on the perpendicular to grain deformation considered. Assuming coniferous wood species and a 3–4% deformation, the slope is 1:1 and for 10% deformation 1:1.5. According to Van der Put, the model may also be applied to situations where the support length is limited but in line with a load on the opposite side of the beam, Fig. 2. Evaluation of additional tests from many literary sources added more credibility to this model, Leijten et al. [5]. It was concluded that the stress dispersion model is superior to any of the previously published empirical models and a potential candidate for introduction in future structural design codes.

2. The stress dispersion model

Models for continuously supported beams that are based on dispersion of the bearing stresses are not new. In 1983, Madsen et al. [6] performed numerical simulations and concluded that the bearing stresses dispersed not beyond 1.5 times the beam depth, which exactly corresponds to what Van der Put [4] derived theoretically, Fig. 2. The same numerical result was later reported

* Corresponding author. Tel.: +31 247 3928; fax: +31 247 0328.
E-mail addresses: a.j.m.leijten@tue.nl (A.J.M. Leijten), a.j.m.jorissen@tue.nl (A.J.M. Jorissen), bjcdeleijer@gmail.com (B.J.C. de Leijer).
[1] Present address: De Groot Vroomshoop, Zwolsekanaal 36, 7681 ED Vroomshoop, The Netherlands.

0950-0618/$ - see front matter © 2011 Elsevier Ltd. All rights reserved.
doi:10.1016/j.conbuildmat.2011.07.022

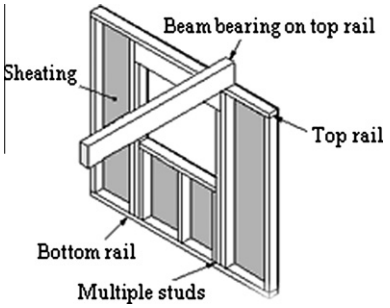

Fig. 1. Load transfer perp to grain.

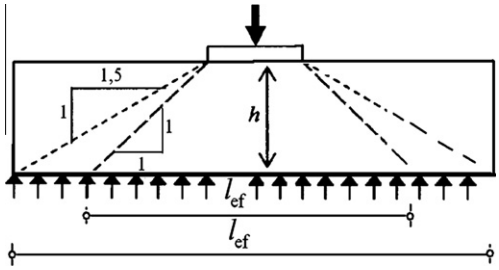

Fig. 2. Continuous supported top loaded beam.

by Riberholt [7] but not used in the model he proposed. Only Van der Put was able to take account of this phenomenon with his analytical stress dispersion model.

As a starting point and reference, the stress dispersion model takes the standard compressive strength, $f_{c,90}$ of a test specimen (prism) loaded over its full surface. For a practical situation, where the loaded area is equal to the beam width, it reads:

$$\frac{F_d}{bl} = \sqrt{\frac{l_{ef}}{l} f_{c,90} k_{c,90} f_{c,0}} \quad (1)$$

where F_d *is* the load, in Newton, l the contact length of the applied load in grain direction in mm, b the width of the beam in mm, l_{ef} the effective stress dispersion length at the support in grain direction in mm and $f_{c,90}$ is the standard compressive strength perpendicular to the grain in N/mm^2.

The Eq. (1) does not apply to the case of beams with a high aspect ratio (beam depth to width), because other types of failure such as rolling shear may occur before the compressive capacity is reached, Basta [8]. A category of beams where the compressive or bearing strength capacity is important, are beams that are not continuously supported as in Fig. 2, but only locally as with the beam in Figs. 1 and 3. The subject of this study concentrates on application of the stress dispersion model for these particular situations.

3. Beams loaded by concentrated loads

There is no difference between the bearing capacity of a beam over a support or under a load plate. In both cases, a force acts on one edge of the beam without finding direct support on the other edge, such as in a simply supported beam loaded by a concentrated load between the end supports. To evaluate the stress dispersion model for concentrated load cases, a research project was carried out by De Leijer [9]. Laboratory experiments were complemented by numerical and optical tests and a summary of his results is presented below.

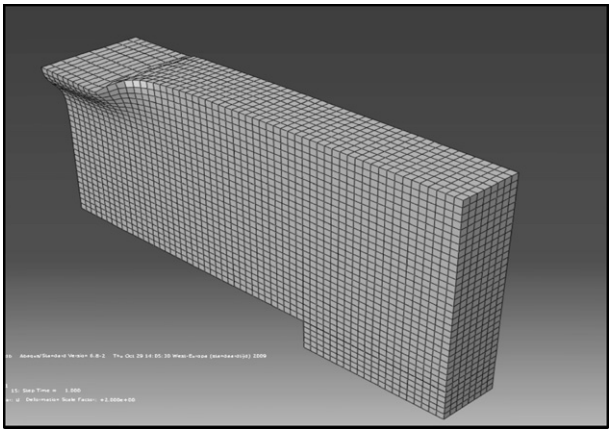

Fig. 3. Symmetrical half of numerical model.

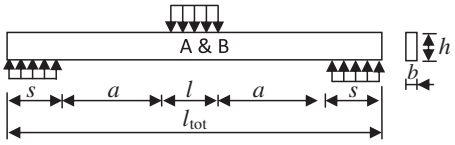

Fig. 4. Sawn timber pieces, Series A and B.

4. Experimental test program

The wood species for all specimens was Nordic Spruce. The mean density and modulus of elasticity was 437 kg/m^3 and 1016 N/mm^2 for the sawn pieces and 447 kg/m^3 and 12538 N/mm^2 for the glued, laminated test pieces respectively. The modulus of elasticity was determined using the Timber Grader by Brookhuis Electronics (based on dynamic wave propagation technology). The grade assigned by the Timber Grader was C24 for the sawn timber and G24h for the glued, laminated pieces. Strength class C24 means a lower 5% fractile or characteristic bending strength and compressive strength perpendicular to grain of 24 N/mm^2 and 2.2 N/mm^2 respectively. This is a standard grade for Scandinavian timber.

Starting point for the lab tests was the simply supported beam loaded by a concentrated load at mid span. The background for the choice of test specimen dimensions was that neither bending nor shear failure should govern but only the bearing capacity. To take a realistic first step the concentrated load at mid span acts over a bearing length of 100 mm in grain direction and over the full beam width. The sawn timber specimens were cut from 145 mm to 220 mm depth and 3000 mm length boards. Two test Series A and B characterized by different depth were produced to span of 590, 880 and 1170 mm respectively, Fig. 4. More details are provided in Table 1. The specimen and span were taken so as to prevent premature failure by shear and bending. Two test Series C and D, were produced with glued, laminated timber, Fig. 5. The depths were from 400 to 600 mm for the same span as the sawn timber Series A and B. More details are provided in Table 2.

5. Numerical modelling, optical verification and laboratory tests

To study and analyse the stress distribution, a FEM program, Abaqus, was used to simulate the behaviour of the test Series, Fig. 3. An 8 node 3D element, C3D8R was used to represent the wood. The material model applied was Hill's criterion which assumes orthotropic behaviour and allows plastic isotropic hardening. Originally, this criterion was developed for isotropic materials like steel and, therefore, no difference is made between tensile and compressive strength. Orthotropic material behaviour is simulated by introducing different tensile and compressive strength values in orthogonal directions. This criterion was chosen as there is no other more suitable material model. Abaques was chosen because of its user friendliness and the available expertise within our research group. An example of the Abaqus model with a deformed load at the top is given in Fig. 3. After initial tuning, the simulations were in agreement with the load–displacement curves of the test on fully surface-loaded standard prismatic compressive

Table 1
Dimensions of sawn timber test Series A and B.

Specimen Series $n = 4$	Width b (mm)	Depth h (mm)	Beam length l_{tot} (mm)	Support s (mm)	a (mm)	Loaded length l (mm)	$(l_{tot} - s)$/depth ratio
A2	40	145	590	100	145	100	3.4
A3			880		290		5.4
A4			1170		435		6.7
B2	40	220	590	100	145	100	2.2
B3			880		290		3.5
B4			1170		435		4.9

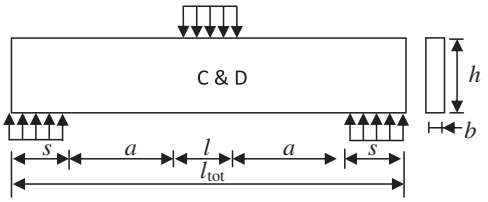

Fig. 5. Glued laminated pieces, Series C and D.

specimens. The simulations continued to consider the test Series A–D. Hill's yield criterion was applied and, despite its shortcomings to represent the timber behaviour in detail, the final results corresponded well with previously reported simulations by Lum and Karacebeyli [10].

6. Indentation depth

The study set out to answer the question as to how the bearing stresses dispersed under a concentrated load. The simulation limits were set by the maximum bending stress of the timber beams or by large crushing of the timber fibres under the concentrated load up to 10% of the beam depth. To analyse the stress dispersion in both parallel to grain and perpendicular to grain directions, the deformation patterns were examined as follows:

To investigate the indentation depth of the perpendicular to grain bearing stresses, the deflection at regular 10 mm spaced cross-sections along the span was evaluated. In Fig. 6 an example is given where the horizontal axis represents the deflection of a test beam with a depth of 145 mm for a vertical concentrated load of 20 kN. It is at this point which the tensile bending strength is reached according to Hill's criterion. On the vertical axes the depth of the cross-section is plotted from the top edge of the beam to 145 mm down to the bottom edge. The maximum deflection is 8.4 mm for the point which is furthest to the right. This point represents the deflection of the top edge fibre at the mid span cross-section (directly under the applied load) which includes the indentation made by the crushing of the fibres. This deformation decreases for fibres that are further from the top to about 2 mm at 50 mm from the top edge. The deflections of subsequent fibres going further down the cross-section remain almost constant as the indentation portion in the deflection has gone. For a cross-section near to the support, there is nearly no deflection at all. This is

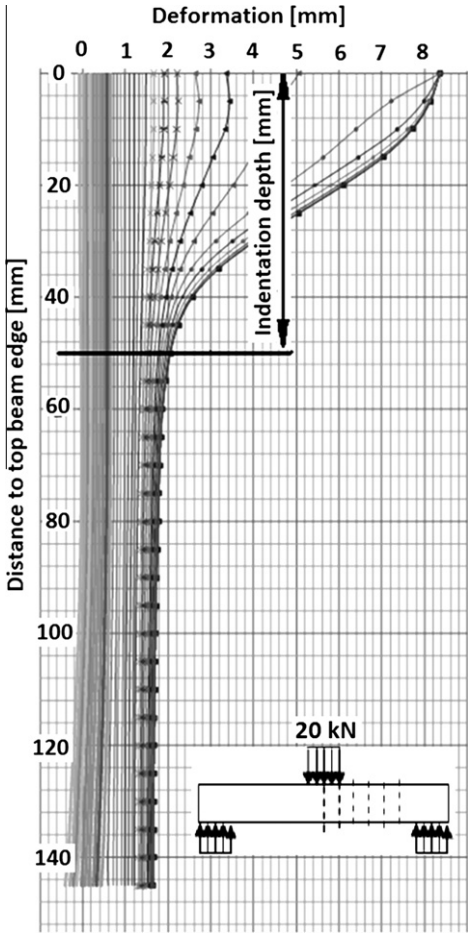

Fig. 6. Penetration depth of bearing stresses in consecutive cross-sections for Series A2-5.

represented by the vertical line which is furthest to the left in Fig. 6. The deflection of some of the near mid span cross-sections also start at 8.4 mm. This is caused by the rigidity of the steel plate under the applied mid span load. A gradual change is noticed for the cross-sections further away from the loaded area as the effect of the indentation decreases. Fibre crushing is approximately max-

Table 2
Dimensions of glued laminated timber test specimen Series C and D.

Specimen Series $n = 4$	Width b (mm)	Depth h (mm)	Beam length l_{tot} (mm)	Support s (mm)	a (mm)	Loaded length l (mm)	$(l_{tot} - s)$/depth ratio
C2	80	400	590	100	145	100	1.2
C3			880		290		2.0
C4			1170		435		2.7
D2	80	600	590	100	145	100	0.8
D3			880		290		1.3
D4			1170		435		1.8

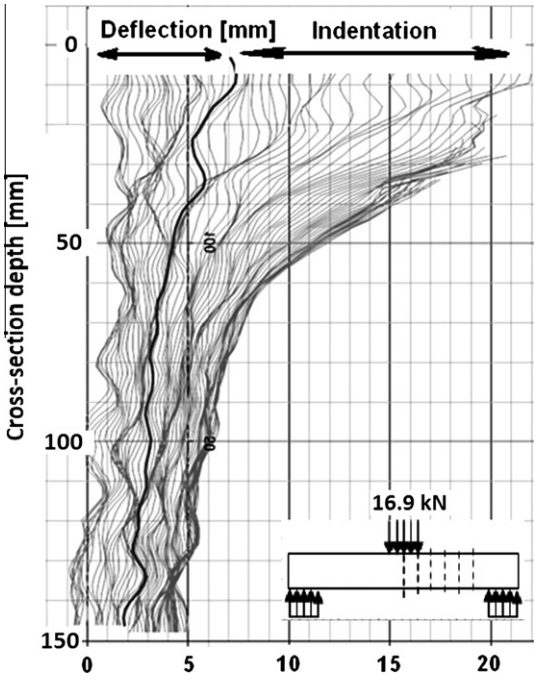

Fig. 7. Results optical detection of indentation depth.

imum 8.4–2.0 = 6.4 mm at the top and is constrained to 50 mm of the beam depth. This is the so-called indentation depth.

For verification of the FEM deformation results, the optical ESPI laser technique was used during the laboratory tests. After some data processing, graphs like Fig. 7 were created. This specific graph originates from Series A2-5 specimen for a load of 16.9 kN. Although the indentation at the top is already more than in Fig. 6 the limited indentation depth compares well. Similar graphs were found for the other specimens. It could be concluded that the indentation depth determined as in Figs. 6 and 7 are quantitatively in good agreement. Both prove that at 50 mm depth in the cross-section, the indentation by bearing stresses perpendicular to grain vanish, and all that remains are bending deflection deformations. This transition is marked in Fig. 7 by a bold line.

As for test Series A, the same numerical procedure was followed and backed up by the optical detection method used for the test Series B–D. The same method of determining the indentation depth was carried out. In Fig. 8, a summary is presented that shows only the mean mid span cross-section deflection per test Series. Although the indentations at the surface increase from 5 mm on

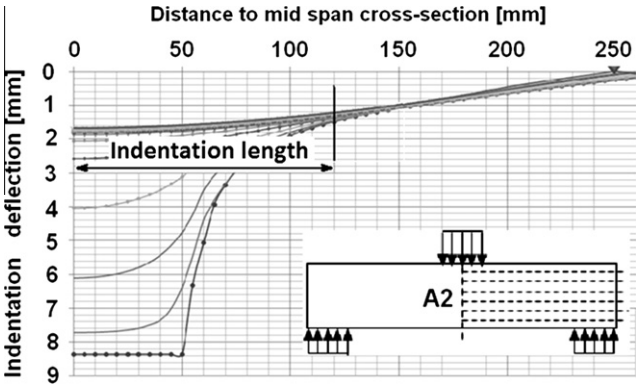

Fig. 9. Indentation length of test A2.

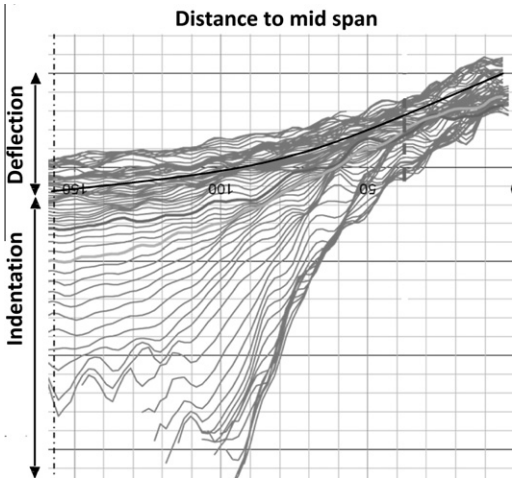

Fig. 10. Optical detection of indentation depth.

the horizontal axis for Series A to 35 mm for the glued laminated test beams of Series D, the indentation depth did not increase with increasing beam depth but attained a maximum of 140 mm for Series C and D.

7. Indentation length

The extent to which the indentation stretches along the grain was analysed in the same way as the indentation depth. Horizontal

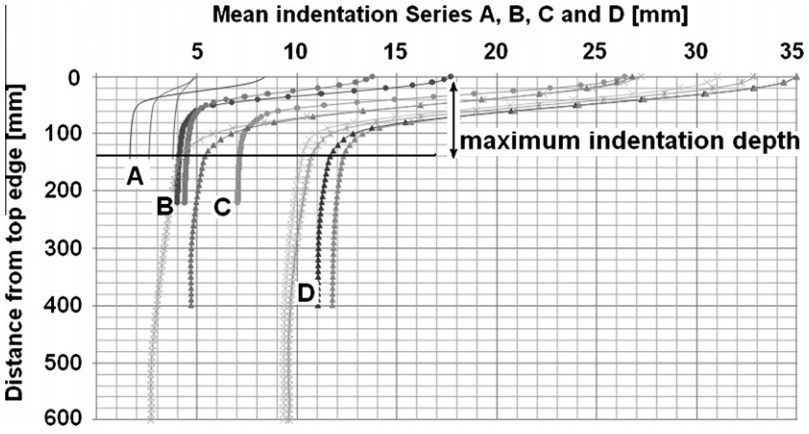

Fig. 8. FEM indentation depths of all test Series.

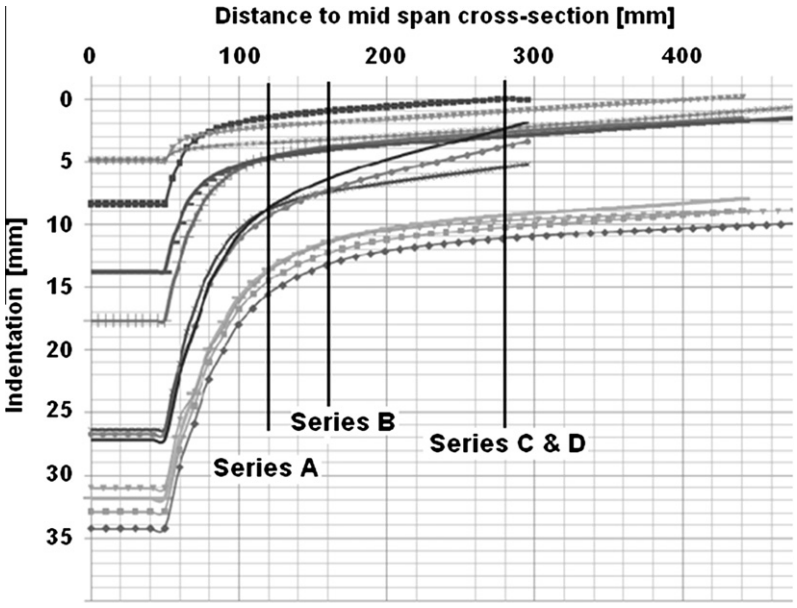

Fig. 11. FEM indentation length all test Series.

Table 3
Overview of mean indentation depth and length and $k_{c,90}$.

Specimen Series		Width b (mm)	Depth h (mm)	Indentation depth, h_e (mm)		Tot. indent. length = l_{ef} (mm)		Dispersion angle ($\tan\alpha$)
Number of tests n				FEM	Test	FEM	Test	FEM
A2	$n = 9$	40	145	50	53	240	233	1.4
A3	$n = 7$			50	67	240	211	1.4
A4	$n = 8$			40	46	240	200	1.75
B2	$n = 9$	40	220	100	100	400	–	1.5
B3	$n = 9$			90	113	320	250*	1.22
B4	$n = 8$			80	87	320	320*	1.38
C2	$n = 8$	80	400	140	140	320	450*	1.36
C3	$n = 8$			140	126	480	560*	1.64
C4	$n = 8$			140	100	560	560*	1.64
D2	$n = 4$	80	600	140	133	560	454*	1.36
D3	$n = 4$			140	132	480	540*	1.57
D4	$n = 4$			140	140	540	560*	1.64
							Mean	1.49

* Reduced number of data reliable.

sections spaced over the depth of the beam show how far the bearing stresses reach outside the loaded area, Fig. 9. The top line represents the bottom fibres which show the deflection of a beam subjected to bending with a maximum of 2 mm at mid span. Consecutive lines represent the deformation of the fibres closer to the top of the beam, clearly showing the increasing indentation. The bottom line of the top beam fibres obviously is straight for 50 mm, which is half the bearing length of the steel plate. Again, at a certain depth, indentation deformations add to the bending deflections. For this particular test, specimen A2-5, the indentation length in grain direction stretches to about 120 mm from mid span to a point where the indentation effect is gone, Fig. 9. These values are observed when the bending tensile stress satisfies Hill's criterion. Similarly, the FEM curves are confirmed by the optical ESPI test technique, Fig. 10. The bolt line shows the deflection when the indentation has disappeared. The same procedure is followed for the other test Series, B–D and an overview is given in Fig. 11. The indentation length is indicated by the vertical lines for each respective test Series. In the same way, it reaches a limit despite the increasing specimen dimensions, are differences is observed for Series C and D.

A comparison between the numerically predicted and optically observed indentation depth and indentation length along the grain shows satisfactory agreement, Table 3. The dispersion angle of the bearing stresses, as shown in Fig. 2, can be derived using the value obtained for the indentation depth and that part of the indentation length that stretches outside the loaded area. This is shown in the

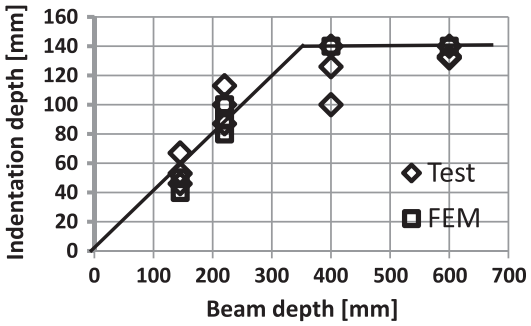

Fig. 12. Comparison FEM and optical results.

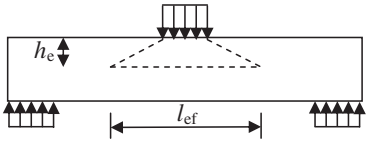

Fig. 13. Effective bearing stresses area.

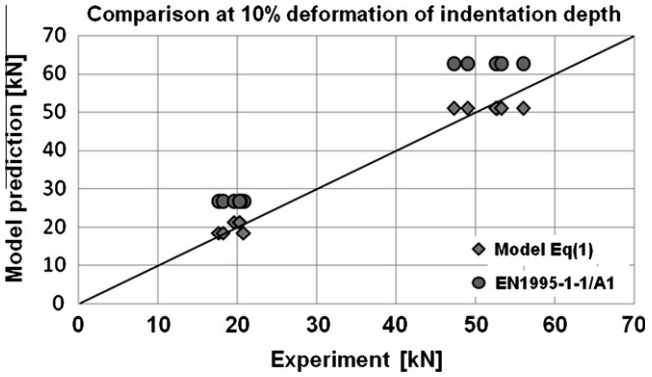

Fig. 14. Model comparison.

last column of Table 3. The mean of these values compare very well with the theoretically derived value of 1.5 by Van der Put [4]. With increasing beam depth for Series C and D the bending deflection become smaller and the optical detection of the boundary of indentation and deflection is more difficult. In other words, in contrast to Series A and B the interpretation of the ESPI test results is not as successful for the Series C and D. Fig. 12 shows the indentation depth versus beam depth for both methods. Because the FEM results correspond well with the optically observed results for the Series A and B, more credit is given to the FEM results than the optical results for Series C and D.

8. Model verification

The stress dispersion model can be applied to the affected area as indicated in Fig. 13. Based on the observed indentation depth, h_e and indentation length, l_{ef} the following can be concluded:

$$h_e = 0.4h \leqslant 140\ \text{mm} \quad (2)$$

$$l_{et} = l + 2x1.5h_e = l + 3h_e \quad (3)$$

The stress dispersion model of Eq. (1) is valid only for the area affected by the indentation. The indentation of the loaded edge fibres of 10% of the indentation depth, are 5.8 mm, 8.8 mm for Series A and B and 14 mm for Series C and D. In Fig. 14, the result of the stress dispersion model is presented as well as the test data. Both are in total agreement. The solid wood data and glued laminated timber data, set with a load at 10% deformation of the dispersion depth of approximately 20 kN and 50 kN respectively, can be distinguished from each other. For comparison, the predictions according to the model given in the amendment Eurocode 5:2008-A1 [11] are given as well. These data point are clearly above the diagonal and may be attained for deformations far beyond 10%. For the sawn timber specimens, Eurocode 5 overestimates the load by 20–40% for Series A and B and 25% for the glued laminated specimens.

9. Conclusion

For non-continuous supported beams loaded perpendicular to grain, it has been shown that the dispersion of bearing stresses are limited to a certain area by using both numerical and optical techniques. For coniferous wood (Spruce), the bearing area is restricted to 40% of the beam depth with a maximum of 140 mm. Applying both stress dispersion model by Van der Put [4], which accounts for this bearing stress area, and the model in Eurocode 5:2008-A1, it is demonstrated that at 10% deformation the bearing stress affected beam depth, which are 5, 8 and 14 mm for solid and glued laminated timber respectively, the stress dispersion model leads to closer agreement to the experimental results.

Acknowledgements

The test have been carried out at the Pieter van Musschenbroeck lab facility of the Faculty with co-operation of lab assistants Eric Wijen, Hans Lamers, Theo Van der Loo, Cor Nanick, Johan Van den Oever, Rien Canters, Martien Ceelen and Rajko Pavic. In addition, a word of thanks for Mary and Raymond Wood for their English language assistance.

References

[1] Kollmann/Côté. Principles of wood science and technology, vol. 1. Springer-Verlag; 1984.
[2] Kühne H. Über den Einfluß von Wassergehalt, Raumgewicht, Faserstellung und Jahrringstellung auf die Festigkeit und Verformbarkeit Scweizerischen Fichten, Tannen, Lärchen, Rotbuchen und Eichenholz, Bericht 183, EMPA, Zürich; 1956.
[3] Gehri E. Timber in compression perpendicular to grain. In: Proceedings of the international conference of IUFRO-S5.02. Copenhagen Denmark, June 16–17, 1997.
[4] Van der Put TACM. Derivation of the bearing strength perpendicular to grain of locally loaded timber blocks. Holz Roh Werkst 2008;66:259–65. doi:10.1007/s00107-008-0234-8.
[5] Leijten AJM, Larsen HJ, Van der Put TCAM. Structural design for compression strength perpendicular to the grain of timber beams. Constr Build Mater 2010;24:252–7. doi:10.1016/j.conbuildmat.2009.08.04.
[6] Madsen B, Hooley RF, Hall CP. A design method for bearing stresses in wood. Can J Civ Eng 1982;9:338–49.
[7] Riberholt H. Compression perpendicular to the grain, Documentation of the strength, COWI –report, June, 2000.
[8] Basta CT. Characterizing perpendicular-to-grain compression in wood construction, Master thesis, Oregon State University, September 21, 2005.
[9] De Leijer BJC. Het loodrecht op druk belasten van de houtvezel bij discreet ondersteunde balken, Master Thesis (in Dutch), Eindhoven University of Technology, 2010-1-CPS/A-2010.2; 2010.
[10] Lum C, Karacebeyli E. Development of the critical bearing design clause in CSA-086.1. In: Proceedings of CIB-W18, paper 27-6-1; 1994.
[11] Eurocode 5/EN1995-1-1/A1. European Committee for Standardization, Management Centre: Rue de Stassart 36, B-1050, Brussels; 2008.